Supplemental Materials for
Polarized localization of phosphatidylserine in endothelium regulates Kir2.1

Claire A. Ruddiman, Richard Peckham, Melissa A. Luse, Yen-Lin Chen, Maniselvan Kuppusamy, Bruce Corliss, P. Jordan Hall, Chien-Jung Lin, Shayn M Peirce, Swapnil K. Sonkusare, Robert P. Mecham, Jessica E. Wagenseil, Brant E. Isakson*

*Corresponding author. Email: brant@virginia.edu

This PDF file includes:

Figs. S1 to S8
Tables S1 to S3

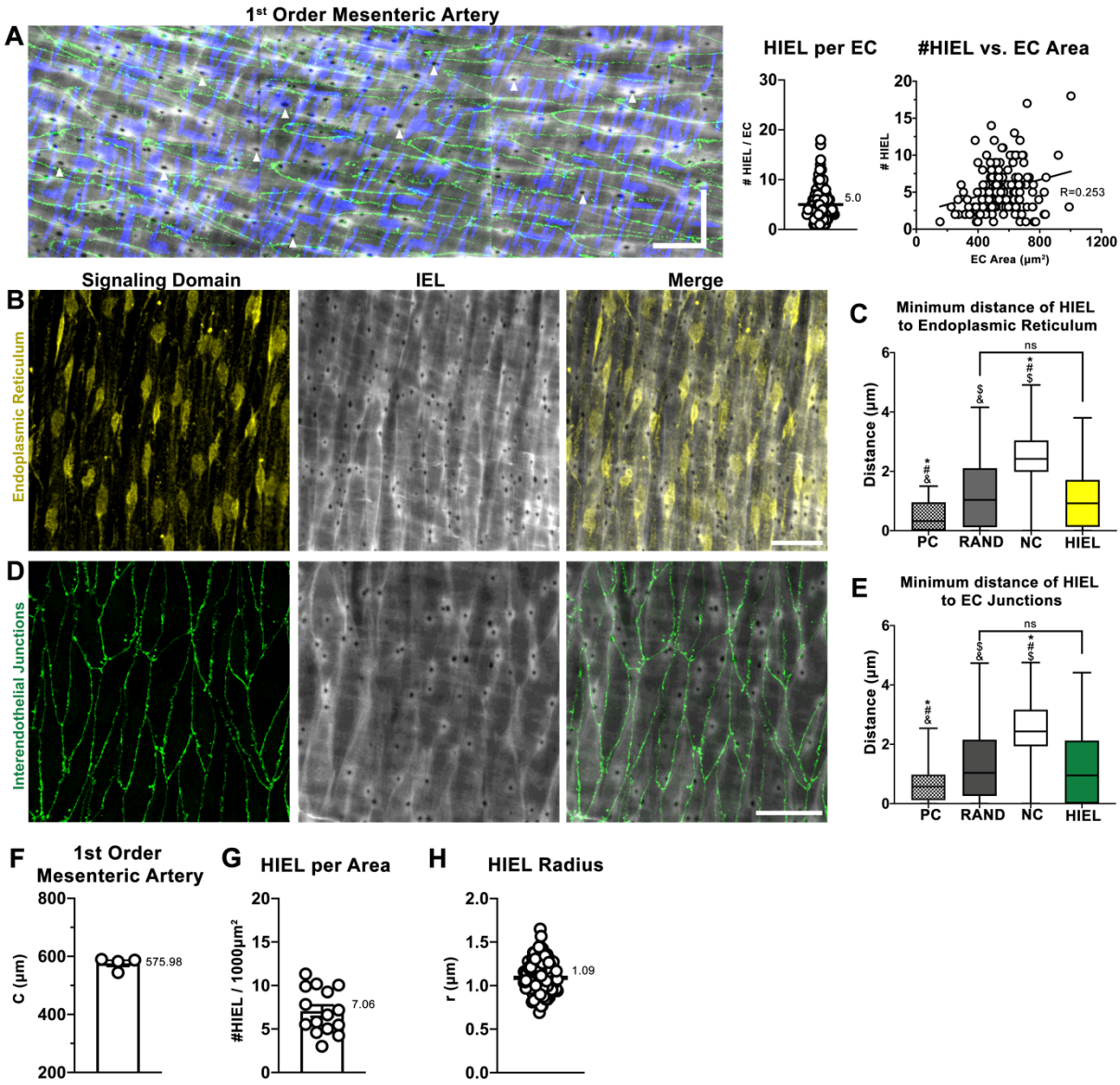

Figure S1: HIEL are randomly distributed with respect to endothelial signaling hubs in first order mesenteric arteries. (A) Representative stitched confocal image of a first order mesenteric artery prepared *en face* and stained for nuclei (blue) via DAPI, the IEL (grey) via Alexa-Fluor 488-linked hydrazide, and interendothelial junctions (green) via claudin-5. Scale bar is 30μm in both directions. Quantification of HIEL per EC and correlation of HIEL per EC versus EC area. N=4 mice, n=4 arteries, n=12 ROIs, and n=155 ECs. (**B**) Representative *en face* confocal image of endoplasmic reticulum (ER, yellow) detected via calnexin and IEL (grey), (**C**) box and whiskers plot of minimum distance of real-world HIEL centers to ER compared to Matlab-simulated HIEL centers. N=1 mouse, n=1 artery, n=2 ROIs, Area= 6.96×10^4 μm^2, and n=315 HIEL. (**D**) Representative *en face* confocal image of interendothelial junctions (green) detected via claudin-5 and IEL (grey), (**E**) box and whiskers plot of minimum distance of real-world HIEL centers to interendothelial junctions compared to Matlab-simulated HIEL centers. N=6 mice, and n=10 arteries, n=15 ROIs, Area=1.66×10^5 μm^2, and n=1200 HIEL. Statistical test: Brown-Forsythe and

Welch ANOVA. # indicates a $p < 0.0001$ significant difference to real-world HIEL distribution, * indicates a $p < 0.0001$ significant difference to RAND, $ indicates a $p < 0.0001$ significant difference to NC distribution, and & indicates a $p < 0.0001$ significant difference to PC. (**F**) Circumference (C) of first order mesenteric arteries measured as the width of the artery in an *en face* preparation. N=4 mice, n=4 arteries. (**G**) HIEL per area taken from *en face* images that were used for HIEL spatial pattern analysis with respect to claudin-5. Number of HIEL was determined via the in-house Matlab program. (**H**) HIEL radius measurements obtained from in-house Matlab program.

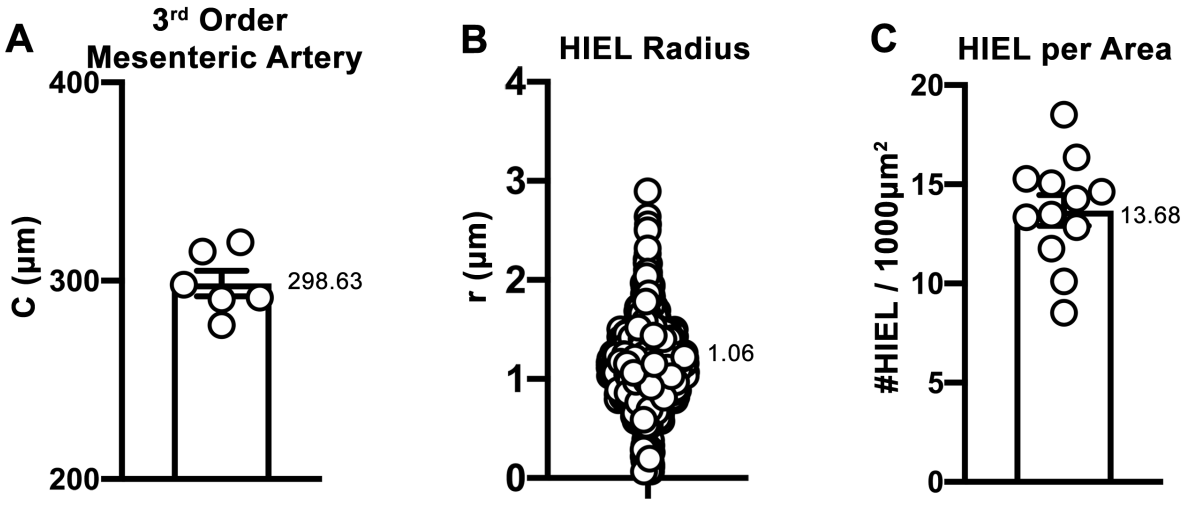

Figure S2: Quantitative data obtained from third order mesenteric artery *en face* preparations. (**A**) Circumference of third order mesenteric arteries measured as the width of the artery in an *en face* preparation. N=5 mouse, n=6 arteries. (**B**) HIEL radius measurements obtained from in-house Matlab program. N=6 mice, and n=10 arteries, n=22 ROIs, Area=$1.48x10^5 \mu m^2$, and n=2166 HIEL. (**C**) HIEL per area taken from *en face* images used in Matlab analysis. Number of HIEL was determined via the in-house Matlab program. N=4 mice, n=4 arteries, n=12 ROIs, and Area=$1.67x10^5\ \mu m^2$.

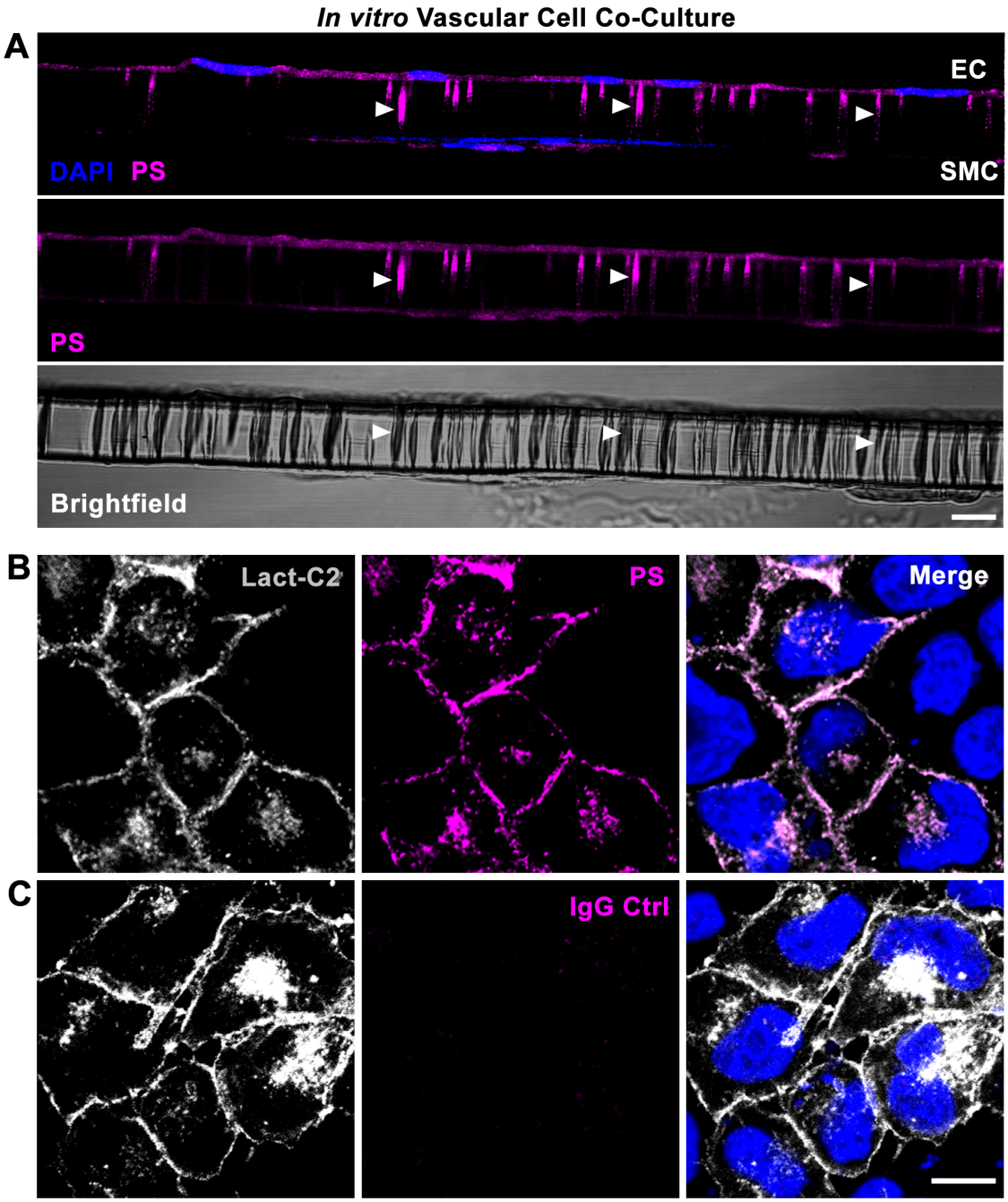

Figure S3: Validation of PS antibody. (A) Transverse cross-sections of an *in vitro* vascular cell co-culture model where EC and SMC are plated on either side of a Transwell. Nuclei (blue) are detected via DAPI and PS (magenta). Brightfield image of Transwell is shown in the bottom panel. Arrowheads indicate PS localization to *in vitro* MEJs. (**B**) HeLa cells transfected with Lact-C2-GFP plasmid (white) and co-stained with PS antibody or (**C**) IgG control. Nuclei (blue) are detected via DAPI. Scale bars are 10μm.

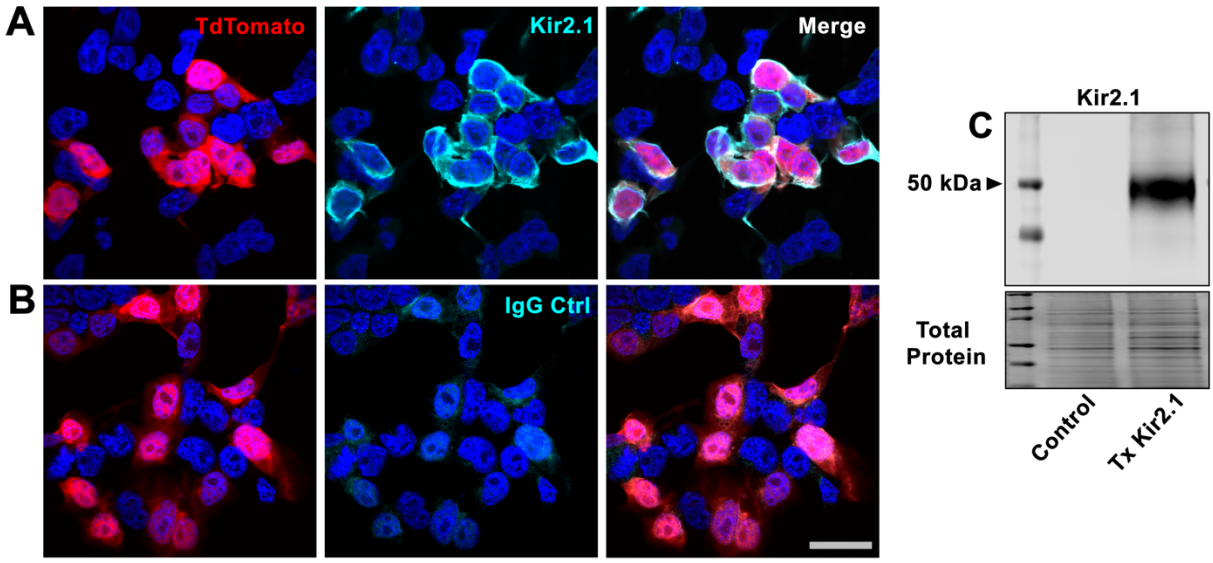

Figure S4: Validation of Kir2.1 antibody. (**A**) HEK293T cells transfected with Kir2.1-T2A-tdTomato plasmid (red) and co-stained with PS antibody or (**B**) IgG control. Nuclei (blue) are detected via DAPI. Scale bar is 30µm. (**C**) Western blot detection of Kir2.1 protein in HEK293T cells that were untreated or transfected with Kir2.1-T2A-tdTomato plasmid. Total protein was used as a loading control.

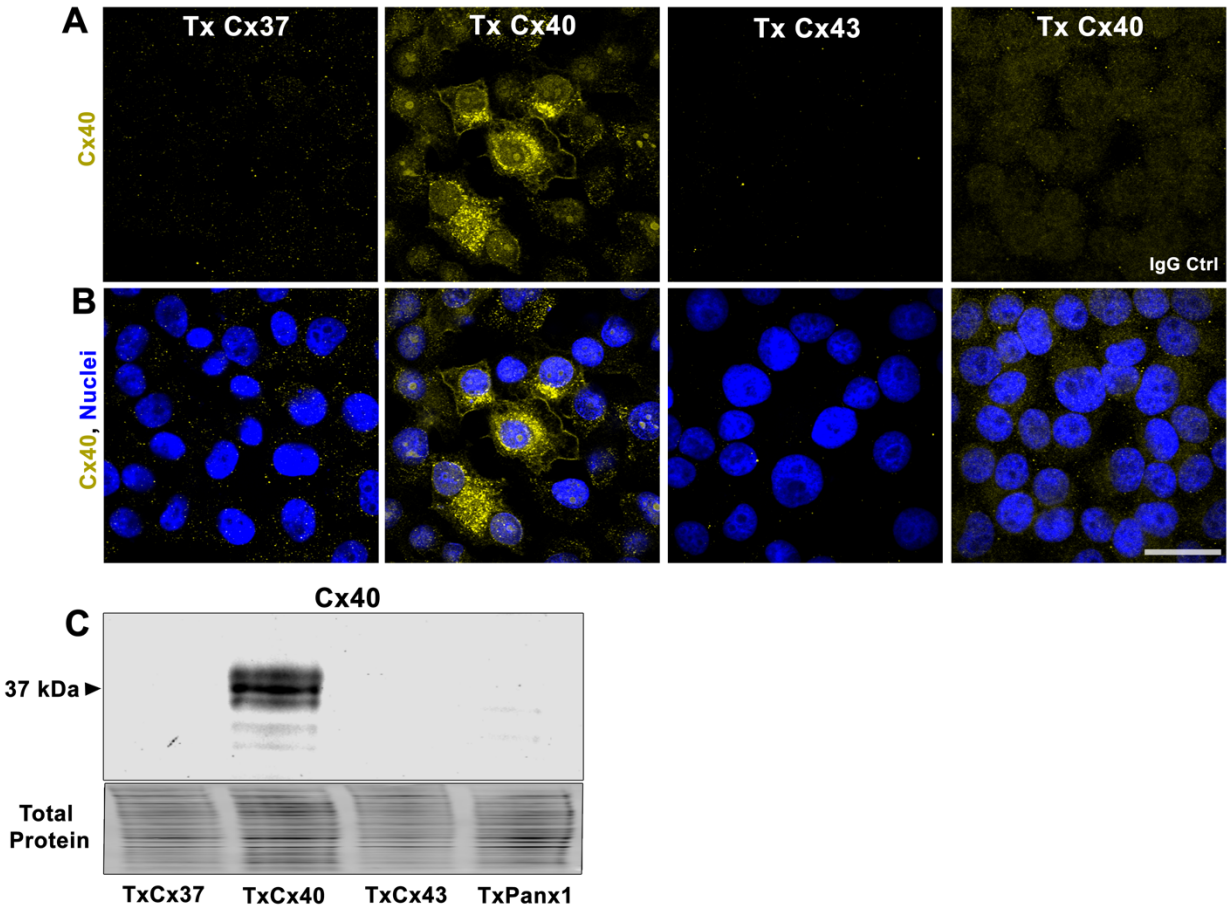

Figure S5: Validation of Cx40 antibody. (**A**) HeLa cells transfected with a connexin plasmid, either connexin 37 (Tx Cx37), connexin 40 (Tx Cx40), or connexin 43 (Tx Cx43), then stained using a Cx40 antibody or IgG control to evaluate Cx40 antibody specificity. Nuclei (blue) are detected via DAPI. Scale bar is 30µm. (**C**) Western blot detection of Cx40 protein in HeLa cells that were transfected with plasmids for Cx37, Cx40, Cx43, and Panx1. Total protein was used as a loading control.

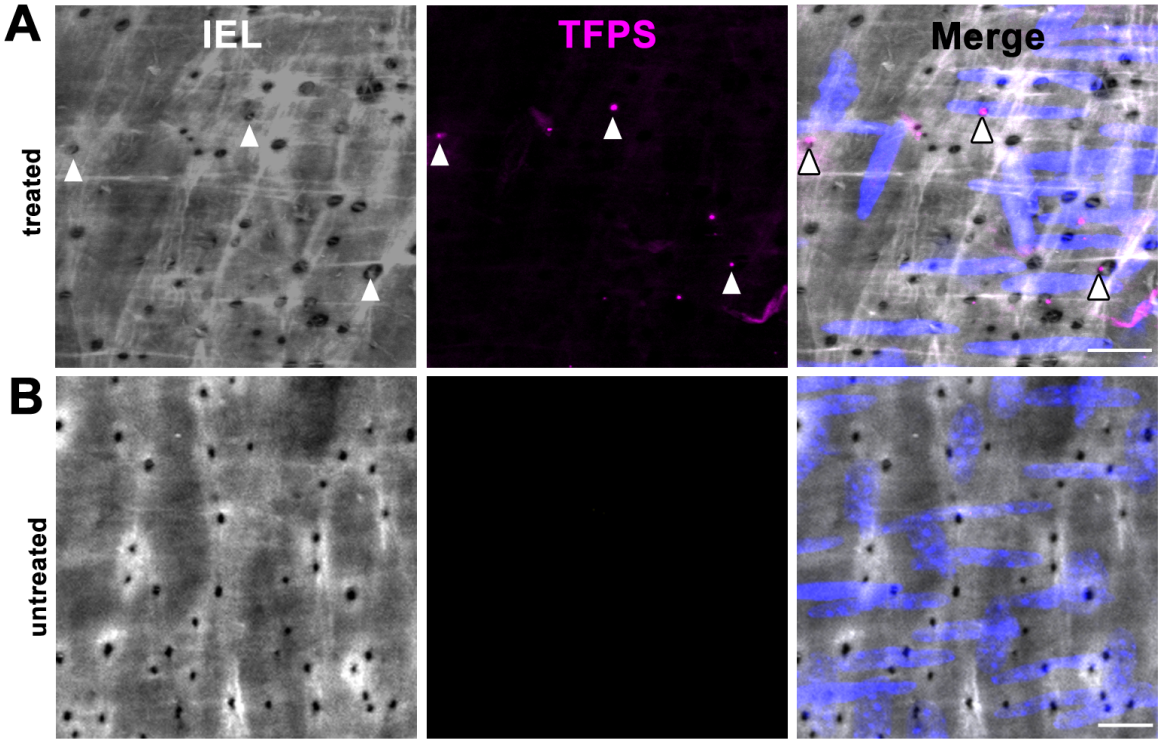

Figure S6: Exogenous application of TopFluor-PS localizes to the MEJ in intact third order mesenteric arteries. Live third order mesenteric arteries prepared *en face* after treatment with (**A**) 10μM TopFluor-PS in the bath solution of a pressure myography setup or (**B**) without treatment. Nuclei (blue) are detected via DAPI and IEL (grey) is detected via Alexa Fluor linked hydrazide. Arrowheads indicate TopFluor-PS localization to MEJ. Scale bars are 10μm.

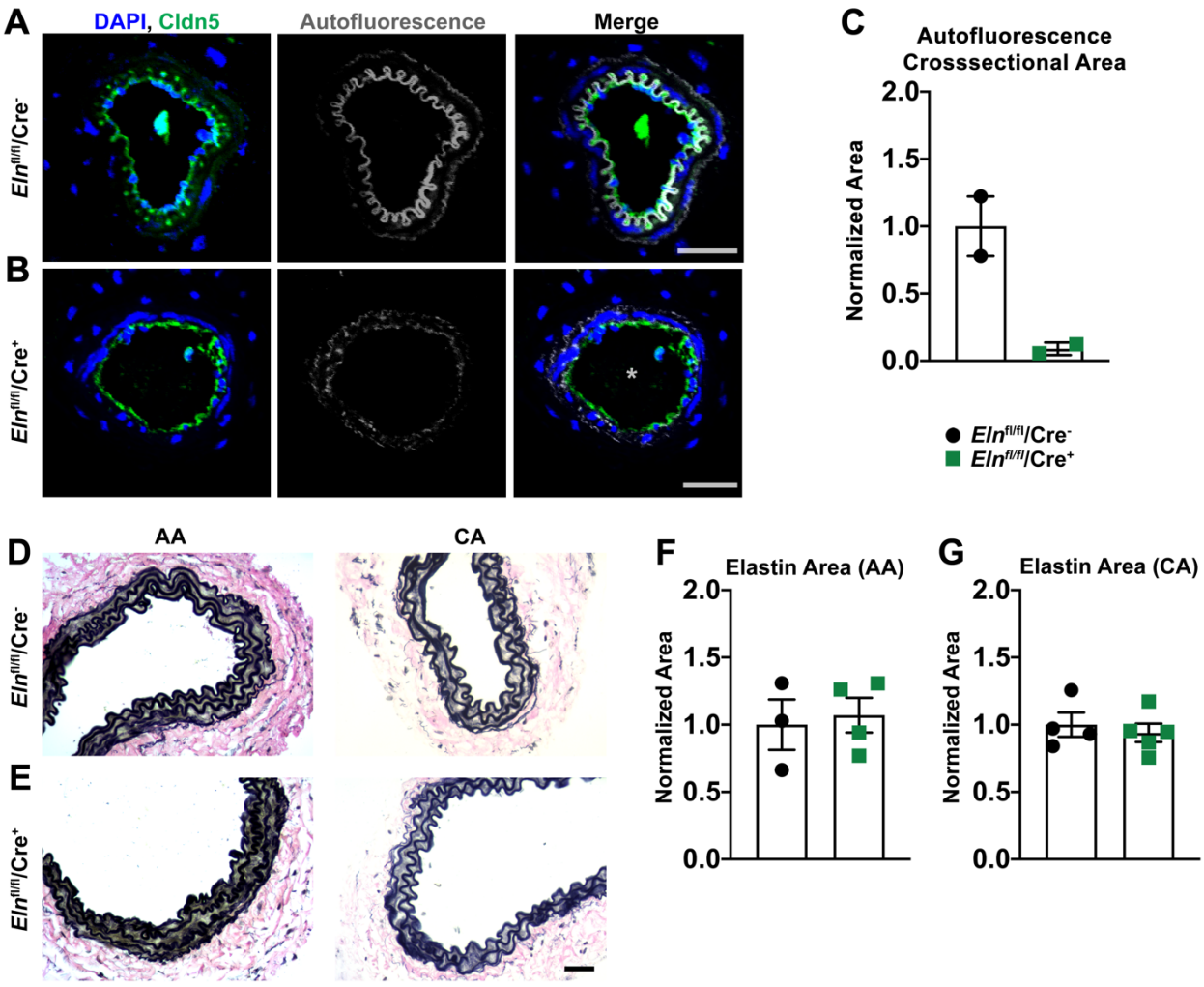

Figure S7: EC-specific knockout of elastin disrupts IEL in resistance arteries and not large conduit arteries. Representative images of cross-sections from third order mesenteric arteries taken from (**A**) *Eln*$^{fl/fl}$/Cre^{-} and (**B**) *Eln*$^{fl/fl}$/Cre^{+} mice where nuclei (blue) are detected via DAPI, IEL (grey) is detected via autofluorescence, and interendothelial junctions (green) are detected via claudin-5. Scale bar is 30µm. N=2 mice per group. (**C**) Quantification of cross-sectional IEL area detected via autofluorescence. Representative images of cross-sections from the abdominal aorta (AA) and carotid artery (CA) of (**D**) *Eln*$^{fl/fl}$/Cre^{-} and (**E**) *Eln*$^{fl/fl}$/Cre^{+} mice. Scale bar is 30µm. Quantification of Verhoeff stain in (**F**) AA and (**G**) CA. N= 3-5 mice per group. Student's t-test.

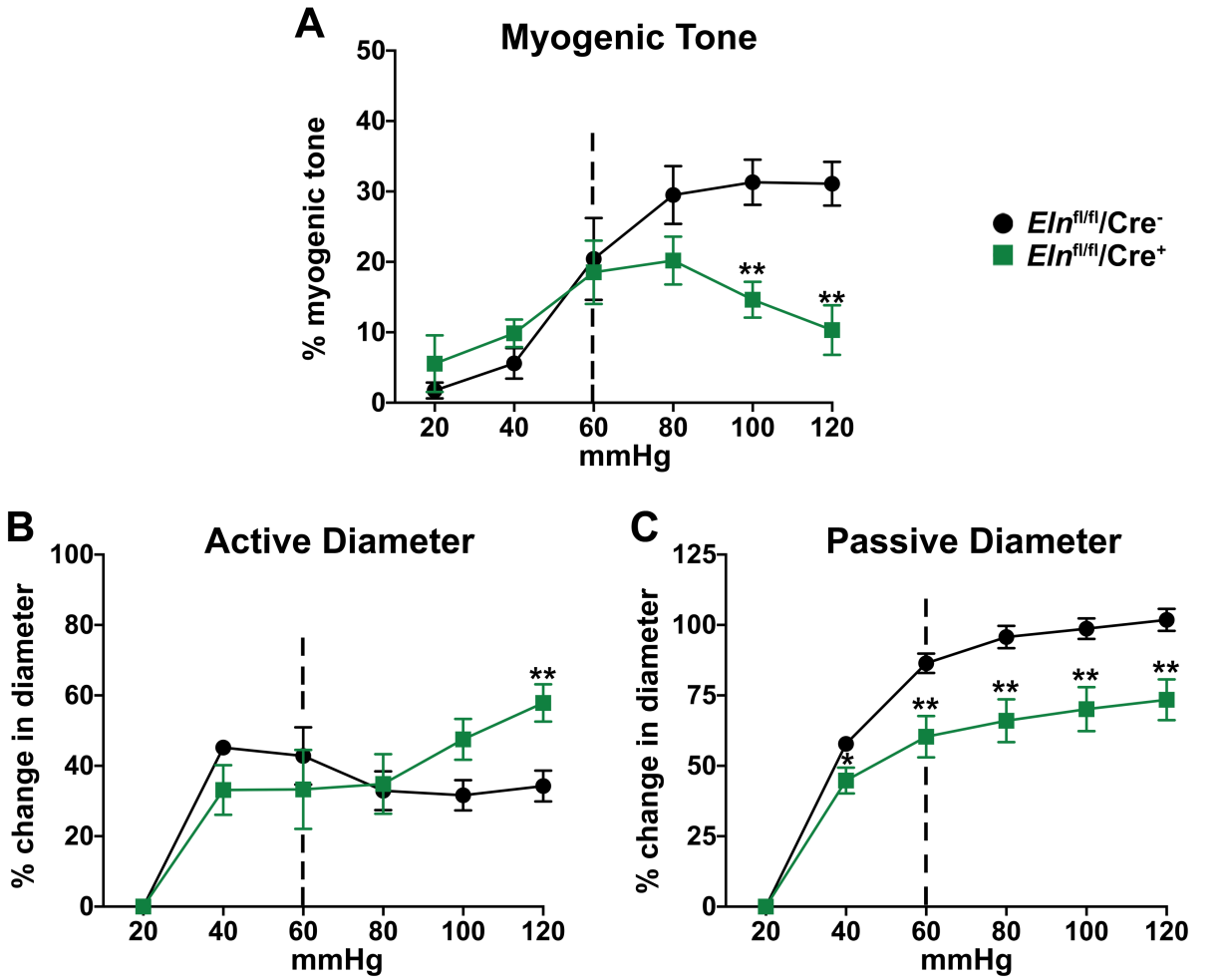

Figure S8: Determination of optimal pressure for myography experiments on *Eln*$^{fl/fl}$/Cre^{+} mice. Pressure myography experiments on third order mesenteric arteries from *Eln*$^{fl/fl}$/Cre^{-} and *Eln*$^{fl/fl}$/Cre^{+} mice, where (**A**) is myogenic tone, (**B**) is the active diameter, and (**C**) is the passive diameter. Dotted line indicates the optimal pressure for *Eln*$^{fl/fl}$/Cre^{+} arteries. N=3 mice per group, n=4-6 arteries per group. Students t-test was performed at each pressure. * indicates $p<0.050$, and ** indicates $p<0.010$.

Variable	Value	Unit	Source	Description
C	298.6	μm	N=4, n=6 arteries **Fig. S2A**	Circumference of 3rd order mesenteric arteries
$\mathbf{C_{IEL}}$	298.6	μm	Assume that it is equal to C	Circumference of IEL
d	2.1	μm	N=5 mice, n=2166 HIEL **Fig. S2B**	Average diameter of HIEL
$\mathbf{\bar{A}_{xy}}$	13,942.9	μm^2	Experimental parameter	Area of en face images
$\mathbf{\tilde{N}_{HIEL}}$	190.7	HIEL / image	N=4, n=4 arteries, n=12 images **Fig. S2C**	Average number of HIEL
$\mathbf{\rho_{HIEL}}$	13.6	HIEL per $1000\mu m^2$	**Eq. 1**	Density of HIEL per $1000\mu m^2$

Table S1: Summary of quantitative data obtained from *en face* images. Measurements taken from third order mesenteric arteries, either manually, automatically via in-house Matlab program, or calculated from direct measurements.

Variable	Value	Units	Source	Description
$\mathbf{Y_{TEM}}$	0.070	μm	Experimental parameter	Thickness of transverse TEM sections
$\mathbf{A_{TEM,1}}$	20.902	μm^2	**Eq. 2**	Artery area spanning $\mathbf{Y_{TEM}}$
$\mathbf{A_{TEM,\,d}}$	627.06	μm^2	**Eq. 4**	Artery area spanning the length **d**
$\mathbf{L_{IEL}}$	1791.6	μm	**Eq. 5**	Length of IEL across 6 TEM sections
$\mathbf{HIEL_{TEM}}$	9	HIEL per A_{TEM}	**Eq. 6**	Number of HIEL expected across $A_{TEM,d}$

Table S2: Calculated parameters of arterial cross-sections imaged via TEM. Experimental and calculated parameters for converting *en face* quantitative data to be interpretable in a TEM geometry.

Case Definition	Variable	Value	Units	Equation	Description
Case1: Maximum case, assumes HIEL are evenly distributed	$D_{HIEL, E}$	54	TEM detections	**Eq. 7**	HIEL detections over 6 sections for Case 1
Case 2: Assumes HIEL are randomly distributed	$D_{HIEL, R}$	32		**Adjusted Eq. 7 (see text)**	HIEL detections over 6 sections for Case 2
Case 3: Minimum case, represents the rare case where each HIEL only appear on 1/6 of sections	$D_{HIEL, S}$	9		**Adjusted Eq. 7 (see text)**	HIEL detections over 6 sections for Case 3
Normalized Case 1	$D_{HIEL, EN}$	30	TEM detections per 1000μm IEL	**Eq. 8**	HIEL detections over 6 sections for Case 1 normalized to IEL length
Normalized Case 2	$D_{HIEL, RN}$	17.8		**Eq. 9**	HIEL detections over 6 sections for Case 2 normalized to IEL length
Normalized Case 3	$D_{HIEL, SN}$	5		**Eq. 10**	HIEL detections over 6 sections for Case 3 normalized to IEL length

Table S3: Case scenarios that consider the potential spatial distributions of HIEL. Prediction of HIEL incidence in TEM sections with consideration of spatial distributions of evenly distributed (**Case 1**), randomly distributed (**Case 2**), or sparsely distributed (**Case 3**). Predictions are then normalized to obtain ratios with respect to IEL length, a metric that can be reproducibly measured in TEM images (**Normalized Cases 1-3**).